DISCRETE AND CONTINUOUS
DYNAMICAL SYSTEMS
Volume **28**, Number **1**, September **2010**

doi:10.3934/dcds.2010.28.xx

pp. **1–XX**

A MATHEMATICAL AND NUMERICAL STUDY OF INCOMPRESSIBLE FLOWS WITH A SURFACTANT MONOLAYER

Yuen-Yick Kwan

Center for Computational Science
Tulane University
New Orleans, LA 70118, USA

Jinhae Park and Jie Shen

Department of Mathematics
Purdue University, 150 N. University Street
West Lafayette, IN 47907-2067, USA

Abstract. We consider in this paper a mathematical model for the incompressible flows with a surfactant monolayer. The presence of surfactant gives rise to coupling surface terms which make the analysis and simulation challenging. We study the well-posedness of this coupled system of PDEs with physically relevant boundary conditions, as well as the stability of a numerical scheme. We also preform numerical simulations by a fast-spectral method and use it to study the effect of surfactant concentration on the motion of an incompressible fluid in a cylinder.

1. **Introduction.** The dynamics of gas/liquid interfaces play an important role in many fields, ranging from biological applications such as lung surfactant therapy [7] and bioreactor [5, 6], to manufacturing applications such as polyurethane foam stabilization [28]. Surfactant monolayers on the gas/liquid interface are ubiquitous in nature and technology. However, the realization of a surfactant-free gas/liquid interface is practically impossible, even in the laboratory [1, 24]. Thus, the modeling of surfactant monolayers on gas/liquid interfaces, and the coupling of bulk flow and the interface in the presence of surfactant monolayers, is very important.

In the present paper, we study a model problem that involves the flow in a cylinder of aspect ratio $\Gamma = H/R$ filled with an incompressible fluid, where H and R are the height and radius of the cylinder, respectively. The flow is driven by the constant rotation of the bottom wall with angular velocity Ω. The cylinder has no lid and a monolayer of insoluble surfactant of concentration c_0 is distributed uniformly on the free surface initially. In fact, experiments were recently conducted by Vogel et al. [33] and Hirsa et al. [11] using vitamin K_1 as the surfactant. For simplicity, we neglect effects due to the surface shear viscosity and surface dilatational viscosity. We also assume that the free surface remains flat. Experimental justifications of these simplifications can be found in [9, 11, 33].

2000 *Mathematics Subject Classification.* Primary: 76B03, 65M70; Secondary: 76R99, 35K55.
Key words and phrases. Existence, Instabilities, Navier-Stokes, Pressure-correction, Spectral-Galerkin method, Surfactant, Weak solution.

Without surfactant, the flow structure of the free-surface flow has been studied experimentally [5, 6, 10, 16, 19, 23, 29, 30, 34], numerically [3, 4, 12, 13, 19, 23], and theoretically [3]. In contrast, there are only a few studies concerning flows with surfactants [11, 23, 33]. In particular, it appears that no three-dimensional simulation for the flow with surfactant is available in the literature. In the present work, we derive the governing equations in the three-dimensional case, prove the global existence of a weak solution, and present three-dimensional numerical simulations using the fast spectral method developed in [14, 15].

The rest of the paper is organized as follows. In Section 2, we introduce the governing equations, derive the relevant boundary conditions and set up the weak formulation. We then derive *a priori* estimates for the coupled system and prove the existence of a weak solution in Section 3. We consider numerical approximations of the coupled system in Section 4 and prove the stability for a semi-discretized (in time) scheme. We present in Section 5 some numerical simulations of the monolayer dynamics. We conclude with some remarks in the last section.

2. **Governing equations.**

2.1. **Basic equations.** The motion of an incompressible fluid in the cylinder, $\mathcal{D} = \{(r,\theta,z) : 0 \le r < 1,\, 0 < z < \Gamma\}$, is governed by the incompressible Navier-Stokes equations

$$\begin{aligned} &\frac{\partial \mathbf{u}}{\partial t} + \mathbf{u}\cdot\nabla\mathbf{u} - \frac{1}{Re}\Delta\mathbf{u} + \nabla p = 0, \\ &\nabla\cdot\mathbf{u} = 0, \end{aligned} \tag{2.1}$$

where $\mathbf{u} = u_r\hat{\mathbf{r}} + u_\theta\hat{\boldsymbol{\theta}} + u_z\hat{\mathbf{z}}$ is the velocity field, and the Reynolds number is defined as $Re = \Omega R^2/\mu$ with μ being the dynamic viscosity coefficient of the fluid. The surfactant concentration is governed by the advection-diffusion equation [31]:

$$\frac{\partial c}{\partial t} + \nabla^s\cdot(c\mathbf{v}) = \frac{1}{Pe^s}\Delta^s c \text{ on } \mathcal{S} = \{(r,\theta,z) : 0 \le r < 1,\, z = \Gamma\},\ \frac{\partial c}{\partial \nu}\Big|_{\partial\mathcal{S}} = 0, \tag{2.2}$$

where c is the surfactant concentration, $\mathbf{v}$ is the restriction of $\mathbf{u}$ on the free surface, $Pe^s = \Omega R^2/D^s$ is the surface Péclect number with D^s being the surface diffusion coefficient of the surfactant, and ∇^s, Δ^s are the surface gradient and Laplacian operators, respectively. Decomposing $\mathbf{v}$ into the components along the surface, $\mathbf{u}^s$, and normal to the surface, $(\mathbf{v}\cdot\mathbf{n})\mathbf{n}$, equation (2.2) can be expressed as

$$\frac{\partial c}{\partial t} + \nabla^s\cdot(c\mathbf{u}^s) + c(\nabla^s\cdot\mathbf{n})(\mathbf{v}\cdot\mathbf{n}) = \frac{1}{Pe^s}\Delta^s c.$$

Since the free surface is assumed to remain flat, we have

$$\mathbf{n} = \hat{\mathbf{z}}, \quad \mathbf{v}\cdot\mathbf{n} = u_z = 0 \text{ on } \mathcal{S}. \tag{2.3}$$

Hence the concentration equation becomes

$$\frac{\partial c}{\partial t} + \nabla^s\cdot(c\mathbf{u}^s) = \frac{1}{Pe^s}\Delta^s c \text{ on } \mathcal{S}. \tag{2.4}$$

2.2. **Stress balance on the surface.** Let $\tilde{\mathcal{S}} \subset \mathcal{S}$ be a surface bounded by a closed curve $\tilde{\mathcal{C}}$. We invoke the balance of surface force

$$\int_{\tilde{\mathcal{S}}} \mathbf{t}(\mathbf{n})\, dA = \int_{\tilde{\mathcal{C}}} \mathbf{t}^s(\boldsymbol{\nu})\, d\ell, \tag{2.5}$$

where $\mathbf{t}(\mathbf{n}) = \mathbf{n} \cdot \mathbf{T}$ is the stress vector representing the contact force per unit area exerted on the surface by the fluid, $\mathbf{T} = -p\mathbf{I} + \mu[\nabla \mathbf{u} + (\nabla \mathbf{u})^T]$ is the stress tensor, $\mathbf{t}^s(\boldsymbol{\nu}) = \boldsymbol{\nu} \cdot \mathbf{T}^s$ is the surface stress vector denoting the contact force per unit length on the curve $\tilde{\mathcal{C}}$, $\boldsymbol{\nu}$ is the outward normal vector to $\tilde{\mathcal{C}}$ on $\mathcal{S}$, and $\mathbf{T}^s$ is the surface stress tensor. We employ the Boussinesq surface fluid model [2, 25, 27] so that the surface stress tensor takes the form

$$\mathbf{T}^s = \sigma \mathbf{I} + (\kappa^s - \mu^s)(\nabla^s \cdot \mathbf{u}^s)\mathbf{I} + \mu^s \left[\nabla^s \mathbf{u}^s + (\nabla^s \mathbf{u}^s)^T\right], \tag{2.6}$$

where σ is the surface tension, κ^s is the surface dilatational viscosity, μ^s is the surface shear viscosity, and ∇^s represents the surface gradient operator. Applying the curl theorem we obtain

$$\int_{\tilde{\mathcal{C}}} \sigma \boldsymbol{\nu}\, d\ell = \int_{\tilde{\mathcal{S}}} \left[\nabla^s \sigma - \sigma \mathbf{n}(\nabla^s \cdot \mathbf{n})\right] dA. \tag{2.7}$$

By neglecting κ^s and μ^s, and combining (2.6) with (2.7), the surface force balance (2.5) becomes

$$\int_{\tilde{\mathcal{S}}} \mathbf{n} \cdot \mathbf{T}\, dA = \int_{\tilde{\mathcal{S}}} \left[\nabla^s \sigma - \sigma \mathbf{n}(\nabla^s \cdot \mathbf{n})\right] dA.$$

Since $\tilde{\mathcal{S}}$ is arbitrary, this results in the surface stress balance equation

$$\mathbf{n} \cdot \mathbf{T} = \nabla^s \sigma - \sigma \mathbf{n}(\nabla^s \cdot \mathbf{n}). \tag{2.8}$$

2.3. **Boundary conditions.** In the cylindrical coordinates, the constant rotation of the bottom is represented by $u_\theta = r$ on $z = 0$. However, this boundary condition for u_θ is incompatible along the edge of the bottom wall $\{(r, \theta, z) : r = 1,\, z = 0\}$ since the side walls are stationary. This singularity for u_θ is due to the mathematical idealization of the physical situation, where there is a thin gap over which u_θ adjusts from 1 on the edge of the bottom wall to 0 on the sidewall. To remove the nonphysical singularity, we replace the boundary condition of u_θ on the bottom wall by a boundary layer function

$$u_\theta(r, \theta, 0) = g(r) := r \left[1 - \exp\left(-\frac{1 - r^2}{\epsilon}\right)\right], \tag{2.9}$$

which converges to the singular boundary condition $u_\theta = r$ outside a boundary layer of width $\mathcal{O}(\epsilon)$. The behavior of this boundary function with $\epsilon = 0.005$ is shown in Figure 1.

With the above modification, the boundary conditions on the bottom and side walls are given by

$$u_r = u_\theta = u_z = 0 \quad \text{on } r = 1, \tag{2.10a}$$
$$u_r = u_z = 0 \quad \text{on } z = 0, \tag{2.10b}$$
$$u_\theta = g(r) \quad \text{on } z = 0, \tag{2.10c}$$

Since the surface is assumed to remain flat, the surface stress balance (2.8) reduces to

$$\hat{\mathbf{z}} \cdot \mathbf{T} = \nabla^s \sigma. \tag{2.11}$$

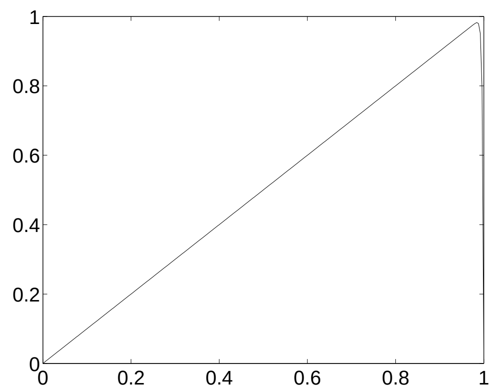

FIGURE 1. Boundary condition (2.9) with $\epsilon = 0.005$.

The tangential components ($\hat{\mathbf{r}}$ and $\hat{\boldsymbol{\theta}}$) are

$$\mu\frac{\partial u_r}{\partial z} = \frac{\partial \sigma}{\partial r}, \quad \mu\frac{\partial u_\theta}{\partial z} = \frac{1}{r}\frac{\partial \sigma}{\partial \theta}. \tag{2.12}$$

Writing equation (2.12) in the dimensionless form, the boundary conditions for the velocity field on the surface are

$$\frac{\partial u_r}{\partial z} = \frac{1}{Ca}\frac{\partial \sigma}{\partial r}, \quad \frac{\partial u_\theta}{\partial z} = \frac{1}{Ca}\frac{1}{r}\frac{\partial \sigma}{\partial \theta}, \quad u_z = 0 \quad \text{on } \mathcal{S}, \tag{2.13}$$

where $Ca = \mu\Omega R/\sigma_0$ is the *capillary number* with σ_0 being the surface tension coefficient of the clear fluid, i.e., a fluid without surfactant.

Conservation of amount of surfactant can be verified by integrating the concentration equation (2.4) over the surface:

$$\frac{d}{dt}\int_{\mathcal{S}} c\,dA + \int_{\partial\mathcal{S}} c\mathbf{u}\cdot\mathbf{n}\,d\ell = \frac{1}{Pe^s}\int_{\partial\mathcal{S}} \frac{\partial c}{\partial \nu}d\ell,$$

where $\boldsymbol{\nu}$ is the outward normal to $\partial\mathcal{S}$. The second term on the left-hand side vanishes because of the boundary condition (2.13), and the term on the right-hand side vanishes thanks to the homogeneous Neumann boundary condition for c (cf. (2.2)).

2.4. **Weak formulation.** Before we state the weak formulation, we first need to introduce some notations.

For $k \in \mathbb{N}$, $p \geq 1$, let $W^{k,p}(\mathcal{R};\mathbf{R}^n)$ denote the Sobolev space of all functions $\mathbf{u} : \mathcal{R} \to \mathbf{R}^n$ satisfying

$$||u||_{W^{k,p}} = \left(\sum_{j=0}^{k}\int_{\mathcal{R}} |\nabla^j \mathbf{u}|^p\,dx\right)^{\frac{1}{p}} < \infty, \quad \mathcal{R} \subset \mathbf{R}^m.$$

We use the standard notation $W^{k,p}(\mathcal{R})$ for $W^{k,p}(\mathcal{R};\mathbf{R})$, and also abuse the notation $W^{k,p}(\mathcal{R})$ to denote $W^{k,p}(\mathcal{R};\mathbf{R}^n)$ when the target space $\mathbf{R}^n$ is clear. Let $(\ ,\ )_{\mathcal{D}}$ and $(\ ,\ )_{\mathcal{S}}$ denote the inner products on $L^2(\mathcal{D})$ and $L^2(\mathcal{S})$ respectively. For simplicity, we use the following notations

$$||f||_{\mathcal{R}} = ||f||_{L^2(\mathcal{R})}, \quad ||f||_{k,\mathcal{R}} = ||f||_{W^{k,2}(\mathcal{R})}, \quad |f|_{k,\mathcal{R}} = ||\nabla^k f||_{L^2(\mathcal{R})}, k \in \mathbb{N},$$

for a function f and a domain $\mathcal{R}$ in $\mathbf{R}^m$. For $A, B > 0$, we use a short notation $A \lesssim B$ to mean that $A \le CB$ for some $C > 0$.

Let us introduce the following functional spaces

$$\begin{aligned}
&\hat{\mathbf{W}} = \left\{\mathbf{u} \in W^{1,2}(\mathcal{D}; \mathbf{R}^3) : \ \mathbf{u} = \mathbf{0} \text{ on } \partial\mathcal{D} \setminus \mathcal{S},\ \mathbf{u}\cdot\mathbf{n} = 0 \text{ on } \mathcal{S}\right\},\\
&\hat{\mathbf{H}} = \left\{\mathbf{u} \in \hat{\mathbf{W}} : \nabla\cdot\mathbf{u} = 0 \text{ in } \mathcal{D}\right\},\\
&\mathbf{W} = \left\{\mathbf{u} = \hat{\mathbf{u}} + \mathbf{g} : \hat{\mathbf{u}} \in \hat{\mathbf{W}}\right\}, \quad \mathbf{H} = \left\{\mathbf{u} = \hat{\mathbf{u}} + \mathbf{g} : \hat{\mathbf{u}} \in \hat{\mathbf{H}}\right\},\\
&V = W^{1,2}(\mathcal{S}; \mathbf{R}),
\end{aligned}$$

where $\mathbf{g}(\mathbf{x}, t) = g(r)\hat{\boldsymbol{\theta}}$, and $g(r)$ is as defined in (2.9). We also define the trilinear form

$$\mathsf{b}(\mathbf{u}, \mathbf{v}, \mathbf{w}) := \int_{\mathcal{D}} (\mathbf{u}\cdot\nabla)\mathbf{u}\cdot\mathbf{w}\, d\mathbf{x}.$$

Since $\nabla\cdot\mathbf{g} = 0$ and $\mathbf{g}\cdot\mathbf{n}|_{\partial\mathcal{D}} = 0$, we have

$$b(\mathbf{u}, \mathbf{v}, \mathbf{v}) = 0 \quad \text{for all } \mathbf{u} \in \mathbf{H},\ \ \mathbf{v} \in W^{1,2}(\mathcal{D}, \mathbf{R}^3). \tag{2.14}$$

For any function space $\mathcal{V}$ with its norm $||\cdot||_{\mathcal{V}}$, and $t > 0$, let $L^p(0, t; \mathcal{V})$ denote the space of all functions $\mathbf{u} : (0, t) \to \mathcal{V}$ satisfying

$$\int_0^t ||\mathbf{u}(s)||^p_{\mathcal{V}} ds < \infty.$$

Then a weak formulation corresponding to the system (2.1)-(2.2) with boundary conditions (2.10) and (2.13) for $\mathbf{u}$ reads:

Find $\hat{\mathbf{u}} \in L^2(0, T; \hat{\mathbf{H}})$ and $c \in L^2(0, T; V)$ so that $\mathbf{u} = \hat{\mathbf{u}} + \mathbf{g}$ and c satisfy

$$\begin{aligned}
&\left(\frac{\partial\mathbf{u}}{\partial t}, \mathbf{v}\right)_{\mathcal{D}} + \mathsf{b}(\mathbf{u}, \mathbf{u}, \mathbf{v}) + \frac{1}{Re}(\nabla\mathbf{u}, \nabla\mathbf{v})_{\mathcal{D}} - \frac{1}{Re\,Ca}(\nabla^s\sigma, \mathbf{v}^s)_{\mathcal{S}} = 0,\\
&\left(\frac{\partial c}{\partial t}, f\right)_{\mathcal{S}} - (c\mathbf{u}^s, \nabla^s f)_{\mathcal{S}} = -\frac{1}{Pe^s}(\nabla^s c, \nabla^s f)_{\mathcal{S}},
\end{aligned} \tag{2.15}$$

for any $\mathbf{v} \in L^2(0, T; \hat{\mathbf{H}})$ and $f \in L^2(0, T; V)$. Note that the extra surface integral in the first equation is the result of integration by parts and (2.13).

3. **Mathematical analysis.**

In this section, we derive *a priori* estimates and prove the existence of a global weak solution for the couple nonlinear system (2.1) and (2.4) with boundary conditions (2.10) and (2.13).

3.1. **A priori estimates.**

Next, we recall the following general interpolation theorem due to Gagliardo and Nirenberg (see [22] and references therein).

Lemma 1 (Gagliardo-Nirenberg)**.** *Let $m \in \mathbb{N}, p, r \in [1, \infty]$, $\mathcal{R} \subset \mathbf{R}^N$, and $u \in W^{m,2}(\mathcal{R}) \cap L^r(\mathcal{R})$. For integer $j \le m$, and $\theta \in [\frac{j}{m}, 1]$ ($\theta \ne 1$ if $m - j - \frac{N}{2} \in \mathbb{N}$), define q by*

$$\frac{1}{q} = \frac{j}{m} + \theta\left(\frac{1}{2} - \frac{m}{N}\right) + \frac{1}{r}(1 - \theta).$$

Then for any $\gamma \in \mathbb{N}^N$, with $|\gamma| = j, \nabla^\gamma u \in L^q(\mathcal{R})$, and satisfies

$$||\nabla^\gamma u||_{L^q(\mathcal{R})} \le C_1 \sum_{|\alpha|=m} ||\nabla^\alpha u||^\theta_{L^2(\mathcal{R})} ||u||^{1-\theta}_{L^r(\mathcal{R})} + C_2||u||_{L^s(\mathcal{R})},$$

where $s = \max\{2, r\}$, $C_1 > 0$, $C_2 \ge 0$ are independent of u. $C_2 = 0$ if $\mathcal{R} = \mathbf{R}^N$.

We note that if $u = 0$ on $\partial\mathcal{R}$, then the above inequality holds with $C_2 = 0$. but in general, it is not possible to take $C_2 = 0$ when $u \neq 0$ on $\partial\mathcal{R}$. As a consequence of the Gagliardo-Nirenberg inequality, we have

$$\begin{aligned} ||u||_{L^4} &\leq C_1 ||u||_{L^2}^{1/2} ||\nabla u||_{L^2}^{1/2} + C_2 ||u||_{L^2} \text{ if } \mathcal{R} \subset \mathbf{R}^2, \\ ||u||_{L^4} &\leq C_1 ||u||_{L^2}^{1/4} ||\nabla u||_{L^2}^{3/4} + C_2 ||u||_{L^2} \text{ if } \mathcal{R} \subset \mathbf{R}^3, \end{aligned} \tag{3.1}$$

for $u \in W^{1,2}(\mathcal{R})$.

It is easy to check that

$$\mathsf{b}(\hat{\mathbf{u}}, \hat{\mathbf{u}}, \mathbf{w}) = \int_{\mathcal{D}} (\hat{\mathbf{u}} \cdot \nabla)\hat{\mathbf{u}} \cdot \mathbf{w} \, d\mathbf{x} = -\mathsf{b}(\hat{\mathbf{u}}, \mathbf{w}, \hat{\mathbf{u}}) \;\; \hat{\mathbf{u}} \in \hat{\mathbf{H}}, \;\; \mathbf{w} \in W^{1,2}(\mathcal{D}, \mathbf{R}^3).$$

By Hölder's inequality, we have the estimate

$$|\mathsf{b}(\hat{\mathbf{u}}, \hat{\mathbf{u}}, \mathbf{w})| \lesssim ||\hat{\mathbf{u}}||_{L^4}^2 |\mathbf{w}|_{1,\mathcal{D}}. \tag{3.2}$$

For any $\mathbf{u} \in \mathbf{H}$ and $\mathbf{w} \in \hat{\mathbf{H}}$, replacing $\mathbf{u}$ by $\hat{\mathbf{u}} + \mathbf{g}$ we get

$$\mathsf{b}(\mathbf{u}, \mathbf{u}, \mathbf{w}) = \mathsf{b}(\hat{\mathbf{u}}, \hat{\mathbf{u}}, \mathbf{w}) + \mathsf{b}(\mathbf{g}, \hat{\mathbf{u}}, \mathbf{w}) + \mathsf{b}(\hat{\mathbf{u}}, \mathbf{g}, \mathbf{w}) + \mathsf{b}(\mathbf{g}, \mathbf{g}, \mathbf{w}).$$

Hence,

$$|\mathsf{b}(\mathbf{u}, \mathbf{u}, \mathbf{w})| \lesssim (||\hat{\mathbf{u}}||_{L^4}^2 + ||\hat{\mathbf{u}}||_{1,\mathcal{D}} + 1) ||\mathbf{w}||_{1,\mathcal{D}}. \tag{3.3}$$

Let

$$\mathbf{X} = \text{closure of } \hat{\mathbf{H}} \text{ in } L^2(\mathcal{D}, \mathbf{R}^3), \quad Y = \text{closure of } V \text{ in } L^2(\mathcal{S}).$$

Then we have the continuous imbeddings

$$\hat{\mathbf{H}} \subset \mathbf{X} \subset \hat{\mathbf{H}}', \;\; V \subset Y \subset V',$$

where M' denotes the dual space of a function space M.

Lemma 2. *If $\mathbf{u} \in L^2(0, T; \mathbf{H})$ and $c \in L^2(0, T; V)$ satisfy (2.15), then $\frac{\partial \hat{\mathbf{u}}}{\partial t} \in L^1(0, T; \hat{\mathbf{H}}')$, $\hat{\mathbf{u}} \in C(0, T; \hat{\mathbf{H}}')$, $\frac{\partial c}{\partial t} \in L^1(0, T; V')$, and $c \in C(0, T; V')$.*

Proof. Using (3.1), (3.3), and Hölder's inequality, we obtain

$$\int_0^T ||(\mathbf{u} \cdot \nabla)\mathbf{u}||_{\hat{\mathbf{H}}'} \, dt \lesssim \int_0^T (||\hat{\mathbf{u}}||_{1,\mathcal{D}}^2 + 1) \, dt < \infty. \tag{3.4}$$

Similarly, we also get

$$\int_0^T ||\Delta \mathbf{u}||_{\hat{\mathbf{H}}'} \, dt \lesssim \int_0^T (||\hat{\mathbf{u}}||_{1,\mathcal{D}}^2 + ||c||_{1,\mathcal{S}}^2 + 1) \, dt < \infty. \tag{3.5}$$

This implies that $\frac{\partial \hat{\mathbf{u}}}{\partial t} \in L^1(0, T; \hat{\mathbf{H}}')$ and consequently $\hat{\mathbf{u}} \in C(0, T; \hat{\mathbf{H}}')$ [21, p. 276].

For any $f \in V$, by the Sobolev imbedding $H^{\frac{1}{2}}(\mathcal{S}) \subset L^4(\mathcal{S})$, the trace theorem, Hölder inequality, and (3.1), we have

$$\begin{aligned} \left| \int_{\mathcal{S}} \nabla^s \cdot (c\mathbf{u}^s) f \right| = \left| \int_{\mathcal{S}} c\mathbf{u}^s \cdot \nabla^s f \right| &\leq ||c||_{L^4(\mathcal{S})} ||\mathbf{u}^s||_{L^4(\mathcal{S})} ||\nabla f||_{L^2(\mathcal{S})} \\ &\lesssim ||\mathbf{u}||_{\frac{1}{2},\partial\mathcal{D}} ||c||_{1,\mathcal{S}} ||f||_{1,\mathcal{S}} \\ &\lesssim ||\mathbf{u}||_{1,\mathcal{D}} ||c||_{1,\mathcal{S}} ||f||_{1,\mathcal{S}}, \end{aligned}$$

$$\int_0^T ||\nabla^s \cdot (c\mathbf{u}^s)||_{V'} dt \lesssim \int_0^T (||\mathbf{u}||_{1,\mathcal{D}}^2 + ||c||_{1,\mathcal{S}}^2) \, dt < \infty.$$

Thus $\frac{\partial c}{\partial t} \in L^1(0, T; V')$ and $c \in C(0, T; V')$. □

In order to prove the global existence of a weak solution, we need to make a reasonable assumption on the equation of state $\sigma(c)$. We shall assume that the equation of state takes the following form:

$$\sigma = \sigma(c) = -\frac{\alpha}{2}c^2 + \kappa(c) \quad \text{with} \quad \alpha > 0,\ \|\kappa'\|^2_{L^\infty} \leq \frac{4\alpha\, Ca}{[C(\mathcal{D}, S)]^2 Pe^s} \tag{3.6}$$

where α can be any positive constant, and $C(\mathcal{D}, S)$ is the constant related to the trace theorem in the following inequality:

$$\|u\|_{\mathcal{S}} \leq C(\mathcal{D}, S)\|u\|_{1,\mathcal{D}}, \tag{3.7}$$

and κ is continuously differentiable with respect to c, i.e., $\kappa \in C^1$. We note that the assumption (3.6) is physically relevant. More precisely, we show in Section 5 that the equation of state used both in [9, 11] and in our simulations is consistent with this assumption.

Theorem 3. *Let $(\mathbf{u}, c)$ be a solution pair of (2.15). If the equation of state $\sigma(c)$ satisfies (3.6), then for any $T > 0$*

$$\max\left\{\int_0^T \left(||\hat{\mathbf{u}}(t)||^2_{1,\mathcal{D}} + ||c(t)||^2_{1,\mathcal{S}}\right) dt, \sup_{0\leq t\leq T}\{||\hat{\mathbf{u}}(t)||_{\mathcal{D}}, ||c(t)||_{\mathcal{S}}\}\right\} \leq K, \tag{3.8}$$

where $\hat{\mathbf{u}} = \mathbf{u} - \mathbf{g}$ and K is a constant depending only on $\mathbf{u}_0$, c_0, and T.

Proof. By taking $\mathbf{v} = \hat{\mathbf{u}}$ in equation (2.15), we obtain

$$\begin{aligned}\frac{d}{dt}\|\hat{\mathbf{u}}\|^2_{\mathcal{D}} + \mathsf{b}(\mathbf{u}, \hat{\mathbf{u}}, \hat{\mathbf{u}}) + \frac{1}{Re}|\hat{\mathbf{u}}|_{1,\mathcal{D}} = \frac{1}{Re\ Ca}(\nabla^s\sigma, \hat{\mathbf{u}}^s)_{\mathcal{S}} - \mathsf{b}(\mathbf{u}, \mathbf{g}, \hat{\mathbf{u}})\\ - \frac{1}{Re}(\nabla\mathbf{g}, \nabla\hat{\mathbf{u}})_{\mathcal{D}}.\end{aligned} \tag{3.9}$$

Since $\sigma = -\frac{\alpha}{2}c^2 + \kappa(c)$ and $\kappa \in C^1$,

$$\frac{1}{Re\ Ca}(\nabla^s\sigma, \hat{\mathbf{u}}^s)_{\mathcal{S}} = -\frac{\alpha}{Re\ Ca}(c\nabla^s c, \hat{\mathbf{u}}^s)_{\mathcal{S}} + \frac{1}{Re\ Ca}(\nabla^s\kappa, \hat{\mathbf{u}}^s)_{\mathcal{S}}. \tag{3.10}$$

Applying Hölder's inequality, Young's inequality and trace theorem, we estimate the second term on the right-hand side of equation (3.10) as

$$\begin{aligned}|(\nabla^s\kappa, \hat{\mathbf{u}}^s)_{\mathcal{S}}| \leq |\hat{\kappa}'|_\infty\|\nabla^s c\|_{\mathcal{S}}\|\hat{\mathbf{u}}^s\|_{\mathcal{S}} \leq \|\kappa'\|_\infty|c|_{1,\mathcal{S}}\|\hat{\mathbf{u}}\|_{1,\mathcal{D}}\\ \leq K_1\left(\eta|c|^2_{1,\mathcal{S}} + \frac{1}{\eta}\|\hat{\mathbf{u}}\|^2_{1,\mathcal{D}}\right),\end{aligned} \tag{3.11}$$

where $K_1 = \|\kappa'\|_{L^\infty}C(\mathcal{D}, \mathcal{S})/2$ with $C(\mathcal{D}, \mathcal{S})$ being the constant in (3.7), and $\eta > 0$ is a constant to be determined. Similarly, we obtain estimates for the second and third terms (3.9) as

$$|\mathsf{b}(\mathbf{u}, \mathbf{g}, \hat{\mathbf{u}})| \leq \|\nabla\mathbf{g}\|_{\infty,\mathcal{D}}\|\mathbf{u}\|_{\mathcal{D}}\|\hat{\mathbf{u}}\|_{\mathcal{D}} \lesssim \|\hat{\mathbf{u}}\|^2_{\mathcal{D}} + \|\mathbf{g}\|^2_{\mathcal{D}},$$

and

$$\left|(\nabla\mathbf{g}, \nabla\hat{\mathbf{u}})_{\mathcal{D}}\right| \leq |\mathbf{g}|_{1,\mathcal{D}}|\hat{\mathbf{u}}|_{1,\mathcal{D}} \leq \varepsilon|\hat{\mathbf{u}}|^2_{1,\mathcal{D}} + C(\varepsilon), \tag{3.12}$$

with $\varepsilon > 0$ to be determined. Thanks to (2.14), we have $\mathsf{b}(\mathbf{u}, \hat{\mathbf{u}}, \hat{\mathbf{u}}) = 0$. Hence

$$\begin{aligned}\frac{d}{dt}\|\hat{\mathbf{u}}\|^2_{\mathcal{D}} + \frac{1}{Re}\left(1 - \varepsilon - \frac{K_1}{\eta Ca}\right)|\hat{\mathbf{u}}|^2_{1,\mathcal{D}} \leq -\frac{\alpha}{Re\ Ca}(c\nabla^s c, \hat{\mathbf{u}}^s)_{\mathcal{S}} + \frac{K_1\eta}{Re\ Ca}|c|^2_{1,\mathcal{S}}\\ + C_1\|\hat{\mathbf{u}}\|^2_{\mathcal{D}} + C_2.\end{aligned} \tag{3.13}$$

On the other hand, replacing f by c in equation (2.15), we get

$$\frac{d}{dt}\|c\|_{\mathcal{S}}^2 + \frac{1}{Pe^s}|c|_{1,\mathcal{S}}^2 = (c\mathbf{u}^s, \nabla^s c)_{\mathcal{S}} = (c\hat{\mathbf{u}}^s, \nabla^s c)_{\mathcal{S}} + (c\mathbf{g}^s, \nabla^s c)_{\mathcal{S}}. \tag{3.14}$$

The last term in (3.14) can be estimated by

$$(c\mathbf{g}^s, \nabla^s c)_{\mathcal{S}} \leq \frac{||\mathbf{g}||_{L^\infty}}{2}\left(\tilde{\varepsilon}|c|_{1,\mathcal{S}}^2 + \frac{1}{\tilde{\varepsilon}}||c||_{\mathcal{S}}^2\right), \tag{3.15}$$

with $\tilde{\varepsilon} > 0$ to be determined. Multiplying (3.14) by $\frac{\alpha}{Re\ Ca}$ and summing up with (3.13), we obtain

$$\begin{aligned} &\frac{d}{dt}\left(||\hat{\mathbf{u}}||_{\mathcal{D}}^2 + \frac{\alpha}{Re\ Ca}||c||_{\mathcal{S}}^2\right) + \frac{1}{Re}\left(1 - \varepsilon - \frac{K_1}{\eta Ca}\right)|\hat{\mathbf{u}}|_{1,\mathcal{D}}^2 \\ &+ \frac{1}{Re\ Ca}\left(\frac{\alpha}{Pe^s} - K_1\eta - \frac{\alpha|\mathbf{g}|_{L^\infty}}{2}\tilde{\varepsilon}\right)|c|_{1,\mathcal{S}}^2 \leq C_1||\hat{\mathbf{u}}||_{\mathcal{D}}^2 + C_2||c||_{\mathcal{S}}^2 + C_3. \end{aligned} \tag{3.16}$$

Under the condition (3.6), we have $K_1^2 < \frac{\alpha Ca}{Pe^s}$. Then there exists $\varepsilon > 0$ satisfying

$$K_1^2 < \frac{\alpha Ca}{Pe^s}(1-\varepsilon).$$

Choose $\eta > 0$ such that

$$\frac{K_1}{Ca(1-\varepsilon)} < \eta < \frac{\alpha}{Pe^s K_1}.$$

Then

$$1 - \varepsilon - \frac{K_1}{\eta Ca} > 0, \quad \frac{\alpha}{Pe^s} - K_1\eta > 0.$$

By taking $\tilde{\varepsilon} > 0$ satisfying

$$\frac{\alpha}{Pe^s} - K_1\eta - \frac{\alpha|\mathbf{g}|_{L^\infty}}{2}\tilde{\varepsilon} > 0,$$

we obtain

$$\frac{d}{dt}\left(||\hat{\mathbf{u}}||_{\mathcal{D}}^2 + ||c||_{\mathcal{S}}^2\right) + \left(|\hat{\mathbf{u}}|_{1,\mathcal{D}}^2 + |c|_{1,\mathcal{S}}^2\right) \leq C_1(||\hat{\mathbf{u}}||_{\mathcal{D}}^2 + ||c||_{\mathcal{S}}^2) + C_2. \tag{3.17}$$

Applying Grönwall's inequality yields

$$||\hat{\mathbf{u}}(t)||_{\mathcal{D}}^2 + ||c(t)||_{\mathcal{S}}^2 \leq \left(||\hat{\mathbf{u}}_0||_{\mathcal{D}}^2 + ||c_0||_{\mathcal{S}}^2\right)e^{C_1 t} + \frac{C_2}{C_1}\left(e^{C_1 t} - 1\right). \tag{3.18}$$

Integrating (3.17) from 0 to T, we have

$$\int_0^T \left(||\hat{\mathbf{u}}(t)||_{1,\mathcal{D}}^2 + ||c(t)||_{1,\mathcal{S}}^2\right) dt \leq K(\mathbf{u}_0, c_0, T).$$

This completes the proof. $\square$

As a consequence, we have the following corollary.

Corollary 4. *If $(\mathbf{u}, c)$ is a solution pair of (2.15) for $T > 0$, then*

$$\hat{\mathbf{u}} \in L^2(0,T;\hat{\mathbf{H}}) \cap L^\infty(0,T;\mathbf{X}),\ c \in L^2(0,T;V) \cap L^\infty(0,T;Y),$$

and moreover,

$$\hat{\mathbf{u}} \in L^{\frac{8}{3}}(0,T;L^4(\mathcal{D})) \cap L^{\frac{10}{3}}((0,T)\times\mathcal{D}),\ c \in L^4(0,T;L^4(\mathcal{S})) = L^4((0,T)\times\mathcal{S}).$$

Proof. It follows from Theorem 3 that

$$\hat{\mathbf{u}} \in L^2(0,T;\hat{\mathbf{H}}) \cap L^\infty(0,T;\mathbf{X}),\ c \in L^2(0,T;V) \cap L^\infty(0,T;Y). \tag{3.19}$$

By inequality (3.1) and $||\hat{\mathbf{u}}||_{\mathcal{D}} < \infty$, we obtain

$$\int_0^T ||\hat{\mathbf{u}}||^p_{L^4(\mathcal{D})}\,dt \lesssim \int_0^T \left(|\hat{\mathbf{u}}|^{\frac{3}{4}}_{1,\mathcal{D}} + 1\right)^p dt \lesssim \int_0^T |\hat{\mathbf{u}}|^{\frac{3p}{4}}_{1,\mathcal{D}}\,dt + 1.$$

Take $p = 8/3$. Then from (3.19),

$$\int_0^T |\hat{\mathbf{u}}|^{\frac{3p}{4}}_{1,\mathcal{D}}\,dt < \infty.$$

Hence $\hat{\mathbf{u}} \in L^{\frac{8}{3}}(0,T;L^4(\mathcal{D}))$. The same argument yields $c \in L^4(0,T;L^4(\mathcal{S})) = L^4((0,T)\times\mathcal{S})$. Applying Hölder's inequality and Poincaré inequality, we obtain that for $p_1 = \frac{n}{2}$, $p_2 = \frac{n}{n-2}$,

$$\begin{aligned}
\int_0^T \int_{\mathcal{D}} |\hat{\mathbf{u}}|^{\frac{2(n+2)}{n}}\,d\mathbf{x}\,dt &\le \int_0^T \left(\int_{\mathcal{D}} |\hat{\mathbf{u}}|^{\frac{4p_1}{n}}\,d\mathbf{x}\right)^{\frac{1}{p_1}} \left(\int_{\mathcal{D}} |\hat{\mathbf{u}}|^{2p_2}\,d\mathbf{x}\right)^{\frac{1}{p_2}} dt \\
&\le \left(\sup_{0\le t\le T} ||\hat{\mathbf{u}}(t)||^{\frac{4}{n}}_{\mathcal{D}}\right) \int_0^T \left(\int_{\mathcal{D}} |\hat{\mathbf{u}}|^{\frac{2n}{n-2}}\,d\mathbf{x}\right)^{\frac{n-2}{n}} dt \\
&\lesssim \left(\sup_{0\le t\le T} ||\hat{\mathbf{u}}(t)||^{\frac{4}{n}}_{\mathcal{D}}\right) \int_0^T \left(\int_{\mathcal{D}} |\nabla\hat{\mathbf{u}}|^2\,d\mathbf{x}\right) dt < \infty.
\end{aligned}$$

Since $\mathcal{D} \subset \mathbf{R}^3$, $\hat{\mathbf{u}} \in L^{\frac{10}{3}}((0,T)\times\mathcal{D})$ with $n = 3$. □

3.2. **Existence of a weak solution.** Having the above results in hand, we are in a position to prove the existence of a weak solution.

Theorem 5. *For any $T > 0$, there exist $\mathbf{u} \in L^2(0,T;\hat{\mathbf{H}})$ and $c \in L^2(0,T;V)$ satisfying (2.15).*

Proof. In order to obtain a weak solution, we use the Galerkin method to approximate (2.15) by a finite-dimensional problem. Let $\{\mathbf{W}_m\}_{m\in\mathbb{N}}$ be an increasing sequence of finite dimensional subspaces of $\hat{\mathbf{H}}$, $\cup_{m\in\mathbb{N}}\mathbf{W}_m = \hat{\mathbf{H}}$, and let $\{\mathbf{w}_1, \mathbf{w}_2, \ldots, \mathbf{w}_m\}$ be an orthonormal basis for $\mathbf{W}_m$. Likewise, we let $\{\mathcal{Z}_m\}_{m\in\mathbb{N}}$ be an increasing sequence of finite dimensional subspaces of V, $\cup_{m\in\mathbb{N}}\mathcal{Z}_m = V$, and $\{z_1, z_2, \cdots, z_m\}$ be an orthonormal basis for $\mathcal{Z}_m$. We now look for an approximate solution to (2.15) in the form

$$\mathbf{u}^m(t) = \sum_{j=1}^m a^m_j(t)\mathbf{w}_j \in \mathbf{W}_m, \quad c^m(t) = \sum_{k=1}^m b^m_k(t) z_k \in \mathcal{Z}_m. \tag{3.20}$$

Plugging $\mathbf{u}^m$ and c^m into (2.15), and taking $\mathbf{v} = \mathbf{w}_i$ and $f = z_j (i,j = 1,2,\ldots,m)$, we obtain an initial value problem for a nonlinear system of ODEs for $\{a^m_j, b^m_j\}^m_{j=1}$. By the standard theory of ODEs, there exists a unique solution on a short interval for each m. We apply the same arguments in Theorem 3 to obtain

$$\max\left\{\int_0^T \left(||\mathbf{u}^m(t)||^2_{1,\mathcal{D}} + ||c^m(t)||^2_{1,\mathcal{S}}\right) dt,\ \sup_{0\le t\le T}\{||\mathbf{u}^m(t)||_{\mathcal{D}}, ||c^m(t)||_{\mathcal{S}}\}\right\} \le K,$$

with a constant K depending only on $\mathbf{u}_0, c_0$, and T. By continuation method, this enables us to extend the solution $(\mathbf{u}^m, c^m)$ on $[0,T)$.

From Corollary 4, $\{\mathbf{u}^m\}_{m=1}^{\infty}$ is a bounded sequence in $L^2(0,T;\hat{\mathbf{H}}) \cap L^\infty(0,T;\mathbf{X})$ and $\{c^m\}_{m=1}^{\infty}$ is a bounded sequence in $L^2(0,T;V) \cap L^\infty(0,T;Y)$. Moreover, it also follows from the Gagliardo-Nirenberg inequality (3.1) that $\{\frac{\partial \mathbf{u}^m}{\partial t}\}$ is bounded in $L^{\frac{4}{3}}(0,T;\hat{\mathbf{H}}')$ and $\{\frac{\partial c^m}{\partial t}\}$ is bounded in $L^{\frac{4}{3}}(0,T;V')$. In fact, using (3.3) and Corollary 4 we have

$$\int_0^T ||((\mathbf{u}^m)^s + \mathbf{g}) \cdot \nabla)((\mathbf{u}^m)^s + \mathbf{g})||_{\hat{\mathbf{H}}'}^{\frac{4}{3}}\, dt \lesssim \int_0^T (||\mathbf{u}^m||_{L^4}^{\frac{8}{3}} + ||\mathbf{u}^m||_{1,\mathcal{D}}^{\frac{4}{3}} + 1)\, dt < \infty.$$

The second integral is finite due to the Gagliardo-Nirenberg inequality (3.1) as in the proof of Corollary 4.

Since $\int_0^T ||\Delta(\mathbf{u}^m + \mathbf{g})||_{\hat{\mathbf{H}}'}^2\, dt < \infty$, $\{\frac{\partial \mathbf{u}^m}{\partial t}\}$ is bounded in $L^{\frac{4}{3}}(0,T;\hat{\mathbf{H}}')$. Since $\sup_{0\le t\le T} ||c^m(t)||_{\mathcal{S}} < \infty$ and $\mathbf{u}^m \in L^2(0,T;\hat{\mathbf{H}})$, as in lemma 2 the Hölder inequality and the inequality (3.1) yield

$$\int_0^T ||\nabla^s \cdot (c^m((\mathbf{u}^m)^s + \mathbf{g}))||_{V'}^{\frac{4}{3}}\, dt \le \int_0^T \left[||c^m||_{L^4(\mathcal{S})} ||(\mathbf{u}^m)^s + \mathbf{g}||_{L^4(\mathcal{S})} \right]^{\frac{4}{3}}\, dt$$

$$\lesssim \int_0^T \left[\left(||\nabla c^m||_{L^2}^{\frac{1}{2}} + 1 \right) ||(\mathbf{u}^m)^s + \mathbf{g}||_{1,\mathcal{D}} \right]^{\frac{4}{3}}\, dt \lesssim \int_0^T ||(\mathbf{u}^m)^s||_{1,\mathcal{D}}^{\frac{4}{3}} ||\nabla^s c^m||_{\mathcal{S}}^{\frac{2}{3}}\, dt + 1$$

$$\le \left(\int_0^T ||\mathbf{u}^m||_{1,\mathcal{D}}^2\, dt \right)^{\frac{2}{3}} \left(\int_0^T ||\nabla^s c^m||_{\mathcal{S}}^2\, dt \right)^{\frac{1}{3}} + 1 < \infty.$$

Hence $\{\frac{\partial c^m}{\partial t}\}$ is bounded in $L^{\frac{4}{3}}(0,T;V')$.

Passing to subsequences if necessary, as $m \to \infty$ we have

$$\begin{aligned}
&\mathbf{u}^m \rightharpoonup \mathbf{u} \text{ weakly in } L^2(0,T;\hat{\mathbf{H}}),\\
&\mathbf{u}^m \rightharpoonup \mathbf{u} \text{ weak* in } L^\infty(0,T;\mathbf{X}),\\
&c^m \rightharpoonup c \text{ weakly in } L^2(0,T;V),\\
&c^m \rightharpoonup c \text{ weak* in } L^\infty(0,T;Y),\\
&\frac{\partial \mathbf{u}^m}{\partial t} \rightharpoonup \frac{\partial \mathbf{u}}{\partial t} \text{ weakly in } L^{\frac{4}{3}}(0,T;\hat{\mathbf{H}}'),\\
&\frac{\partial c^m}{\partial t} \rightharpoonup \frac{\partial c}{\partial t} \text{ weakly in } L^{\frac{4}{3}}(0,T;V').
\end{aligned}$$

By Aubin's compactness lemma (see [22, p. 363] and references therein), we have

$$\begin{aligned}
&\mathbf{u}^m \to \mathbf{u} \text{ strongly in } L^2(0,T;\mathbf{X}) \text{ as } m \to \infty,\\
&c^m \to c \text{ strongly in } L^2(0,T;Y) \text{ as } m \to \infty.
\end{aligned}$$

Together with Corollary 4, it is standard to show that $(\mathbf{u}, c)$ is a weak solution pair (see [21, p. 334] or [32]). This completes the proof. □

4. **Numerical schemes.**

In this section, we shall construct numerical schemes for the system (2.15). To simplify the presentation, we start with a first-order pressure-correction (semi-discretized in time) scheme and prove its stability. The proof can be carried over to second-order pressure-correction schemes, albeit technically tedious. Then, we describe in some detail the full discretization scheme which is based on the second-order rotational pressure-correction scheme [8] in time and a spectral-Galerkin method [26] in space.

4.1. **Stability of a time discretization.** We consider the following first-order pressure-correction semi-implicit Euler scheme: Given $\mathbf{u}_0 \in \mathbf{H}$, $c_0 \in V$ and $p_0 \in L^2(\mathcal{D})$, define recursively $\tilde{\mathbf{u}}_n \in \mathbf{W}$, $c_n \in V$ and $(p_n, \mathbf{u}_n)$ by

$$\frac{1}{\Delta t}(\tilde{\mathbf{u}}_n - \mathbf{u}_{n-1}, \mathbf{v})_{\mathcal{D}} + \mathsf{b}(\mathbf{u}_{n-1}, \tilde{\mathbf{u}}_n, \mathbf{v}) + \frac{1}{Re}(\nabla \tilde{\mathbf{u}}_n, \nabla \mathbf{v})_{\mathcal{D}} - (p_{n-1}, \nabla \cdot \mathbf{v})_{\mathcal{D}}$$
$$+ \frac{\alpha}{Re\,Ca}(c_{n-1}\nabla^s c_n, \mathbf{v}^s)_{\mathcal{S}} - \frac{1}{Re\,Ca}(\nabla^s \kappa_{n-1}, \mathbf{v}^s)_{\mathcal{S}} = 0, \quad \forall \mathbf{v} \in \hat{\mathbf{W}}, \tag{4.1a}$$
$$\frac{1}{\Delta t}(c_n - c_{n-1}, f)_{\mathcal{S}} - (c_{n-1}\mathbf{u}_n^s, \nabla^s f)_{\mathcal{S}} = -\frac{1}{Pe^s}(\nabla^s c_n, \nabla^s f), \quad \forall f \in V, \tag{4.1b}$$
$$\frac{1}{\Delta t}(\mathbf{u}_n - \tilde{\mathbf{u}}_{n-1}) + \nabla(p_n - p_{n-1}) = 0, \;\; \nabla \cdot \mathbf{u}_n = 0, \;\; \mathbf{u}_n \cdot \mathbf{n}|_{\partial\mathcal{D}} = 0. \tag{4.1c}$$

We note that in the above scheme, (4.1a)-(4.1b) forms a coupled **linear elliptic** system for $(\tilde{\mathbf{u}}_n, c_n)$, while $(p_n, \mathbf{u}_n)$ can be obtained from (4.1c), which is a usual projection step, by solving a Poisson equation. Moreover, we show below that this scheme is essentially unconditionally stable. Hence, the above scheme is very efficient when coupled with a spacial discretization with efficient elliptic solvers.

Theorem 6. *Let $(\{\tilde{\mathbf{u}}_n\}, \{\mathbf{u}_n\}, \{c_n\}, \{p_n\})$ be the solutions of the scheme (4.1). Under the assumption (3.6), there exists $C > 0$ such that for all $\Delta t \le C$, we have*

$$\|\hat{\mathbf{u}}_N\|_{\mathcal{D}}^2 + \|c_N\|_{\mathcal{S}}^2 + \Delta t\|\nabla p_N\|^2 + \Delta t \sum_{n=0}^{N}\left(|\hat{\tilde{\mathbf{u}}}_n|_{1,\mathcal{D}}^2 + |c_n|_{1,\mathcal{S}}^2\right) \le K(\mathbf{u}_0, c_0, p_0), \;\; \forall N \le \frac{T}{\Delta t},$$

where $\hat{\mathbf{u}}_n = \mathbf{u}_n - \mathbf{g}$, $\hat{\tilde{\mathbf{u}}}_n = \tilde{\mathbf{u}}_n - \mathbf{g}$ and K is a constant depending only on $\mathbf{u}_0$, c_0 and p_0.

Proof. Replacing $\mathbf{v}$ by $\hat{\tilde{\mathbf{u}}}_n = \tilde{\mathbf{u}}_n - \mathbf{g}$ in equation (4.1a) yields

$$\frac{1}{2\Delta t}\left(\|\hat{\tilde{\mathbf{u}}}_n\|_{\mathcal{D}}^2 - \|\hat{\mathbf{u}}_{n-1}\|_{\mathcal{D}}^2 + \|\hat{\tilde{\mathbf{u}}}_n - \hat{\mathbf{u}}_{n-1}\|_{\mathcal{D}}^2\right) + \frac{1}{Re}|\hat{\tilde{\mathbf{u}}}_n|_{1,\mathcal{D}}^2 - (p_{n-1}, \nabla \cdot \hat{\tilde{\mathbf{u}}}_n)_{\mathcal{D}}$$
$$+ \frac{\alpha}{Re\,Ca}(c_{n-1}\nabla^s c_n, \hat{\tilde{\mathbf{u}}}_n^s)_{\mathcal{S}} = \frac{1}{Re\,Ca}(\nabla^s \kappa_{n-1}, \hat{\tilde{\mathbf{u}}}_n^s)_{\mathcal{S}} - \mathsf{b}(\mathbf{u}_{n-1}, \mathbf{g}, \hat{\tilde{\mathbf{u}}}_n)$$
$$- \frac{1}{Re}(\nabla \mathbf{g}, \nabla \hat{\tilde{\mathbf{u}}}_n)_{\mathcal{D}}. \tag{4.2}$$

The second term on the right-hand side can be estimated by using Cauchy-Schwarz and Poincaré inequalities as follows:

$$|\mathsf{b}(\mathbf{u}_{n-1}, \mathbf{g}, \hat{\tilde{\mathbf{u}}}_n)| \le \|\nabla \mathbf{g}\|_{\infty,\mathcal{D}}\|\mathbf{u}_{n-1}\|_{\mathcal{D}}\|\hat{\tilde{\mathbf{u}}}_n\|_{\mathcal{D}} \le C_0\|\hat{\mathbf{u}}_{n-1}\|_{\mathcal{D}}^2 + \varepsilon_1|\hat{\tilde{\mathbf{u}}}_n|_{1,\mathcal{D}}^2.$$

The other terms on the right-hand side can be bounded as in equations (3.11) and (3.12) to obtain

$$\frac{1}{2\Delta t}\left(\|\hat{\tilde{\mathbf{u}}}_n\|_{\mathcal{D}}^2 - \|\hat{\mathbf{u}}_{n-1}\|_{\mathcal{D}}^2 + \|\hat{\tilde{\mathbf{u}}}_n - \hat{\mathbf{u}}_{n-1}\|_{\mathcal{D}}^2\right) + \frac{1}{Re}\left(1 - \varepsilon_1 - \varepsilon - \frac{K_1}{\eta Ca}\right)|\hat{\tilde{\mathbf{u}}}_n|_{1,\mathcal{D}}^2$$
$$- (p_{n-1}, \nabla \cdot \hat{\tilde{\mathbf{u}}}_n)_{\mathcal{D}} + \frac{\alpha}{Re\,Ca}(c_{n-1}\nabla^s c_n, \hat{\tilde{\mathbf{u}}}_n^s)_{\mathcal{S}}$$
$$\le \frac{K_1\eta}{Re\,Ca}|c_n|_{1,\mathcal{S}}^2 + C_1\|\hat{\mathbf{u}}_{n-1}\|_{\mathcal{D}}^2 + C_2. \tag{4.3}$$

Next, we rearrange (4.1c) into

$$\frac{1}{\sqrt{\Delta t}}\hat{\mathbf{u}}_n + \sqrt{\Delta t}\nabla p_n = \frac{1}{\sqrt{\Delta t}}\hat{\tilde{\mathbf{u}}}_n + \sqrt{\Delta t}\nabla p_{n-1}$$

and taking the inner product of the above equation with itself on both sides, we obtain

$$\frac{1}{\Delta t}\|\hat{\mathbf{u}}_n\|^2_{\mathcal{D}} + \Delta t\|\nabla p_n\|^2_{\mathcal{D}} = \frac{1}{\Delta t}\|\hat{\tilde{\mathbf{u}}}_n\|^2_{\mathcal{D}} + \Delta t\|\nabla p_{n-1}\|^2_{\mathcal{D}} - 2(p_{n-1}, \nabla\cdot\hat{\tilde{\mathbf{u}}}_n)_{\mathcal{D}}. \quad (4.4)$$

On the other hand, taking f by c_n in (4.1b) yields

$$\begin{aligned}\frac{1}{2\Delta t}\left(\delta\|c_n\|^2_{\mathcal{S}} + \|\delta c_n\|^2_{\mathcal{S}}\right) + \frac{1}{Pe^s}|c_n|^2_{1,\mathcal{S}} &= (c_{n-1}\mathbf{u}^s_n, \nabla^s c_n)_{\mathcal{S}} \\ &= (c_{n-1}\hat{\mathbf{u}}^s_n, \nabla^s c_n)_{\mathcal{S}} + (c_{n-1}\mathbf{g}^s, \nabla^s c_n)_{\mathcal{S}}, \quad (4.5)\end{aligned}$$

where we have used the short-hand notation: $\delta v_n = v_n - v_{n-1}$ for any sequence $\{v_k\}$. The right-hand side can be bounded similar to equation (3.15).

Multiplying equation (4.5) by $\frac{\alpha}{Re\,Ca}$, equation (4.4) by $\frac{1}{2}$ and summing up with equation (4.3), and taking η, ε and $\tilde{\varepsilon}$ as in Theorem 3, we obtain

$$\begin{aligned}&\frac{1}{2\Delta t}\delta\left(\|\hat{\mathbf{u}}_n\|^2_{\mathcal{D}} + \frac{\alpha}{Re\,Ca}\|c_n\|^2_{\mathcal{S}}\right) + C_3\left(|\hat{\tilde{\mathbf{u}}}_n|^2_{1,\mathcal{D}} + \frac{\alpha}{Re\,Ca}|c_n|^2_{1,\mathcal{S}}\right) + \frac{1}{2}\Delta t\,\delta\|\nabla p_n\|^2_{\mathcal{D}} \\ &\quad \le C_4(\|\hat{\mathbf{u}}_{n-1}\|^2_{\mathcal{D}} + \|c_{n-1}\|^2_{\mathcal{S}} + \|c_n\|^2_{\mathcal{S}} + 1). \quad (4.6)\end{aligned}$$

We can then conclude by applying the discrete Grönwall lemma. □

4.2. **A second-order time discretization.** The scheme (4.1) can be easily extended to second-order in time. We now describe a second-order version, which is based on the second-order rotational pressure-correction scheme, that we use in our simulation.

$$\begin{aligned}&\frac{1}{2\Delta t}(3\tilde{\mathbf{u}}_n - 4\mathbf{u}_{n-1} + \mathbf{u}_{n-2}, \mathbf{v})_{\mathcal{D}} + \mathsf{b}(\mathbf{u}^*_n, \tilde{\mathbf{u}}_n, \mathbf{v}) + \frac{1}{Re}(\nabla\tilde{\mathbf{u}}_n, \nabla\mathbf{v})_{\mathcal{D}} - (p_{n-1}, \nabla\cdot\mathbf{v})_{\mathcal{D}} \\ &\quad + \frac{\alpha}{Re\,Ca}(c^*_n\nabla^s c_n, \mathbf{v}^s)_{\mathcal{S}} - \frac{1}{Re\,Ca}(\nabla^s\kappa^*_n, \mathbf{v}^s)_{\mathcal{S}} = 0, \quad \forall v \in \hat{\mathbf{W}}, \quad (4.7a)\end{aligned}$$

$$\frac{1}{2\Delta t}(3c_n - 4c_{n-1} + c_{n-2}, f)_{\mathcal{S}} - (c^*_n\mathbf{u}^s_n, \nabla^s f)_{\mathcal{S}} = -\frac{1}{Pe^s}(\nabla^s c_n, \nabla^s f), \quad \forall f \in V, \quad (4.7b)$$

$$\frac{3}{2\Delta t}(\mathbf{u}_n - \tilde{\mathbf{u}}_{n-1}) + \nabla(p_n - p_{n-1} + \frac{1}{Re}\nabla\cdot\tilde{\mathbf{u}}_n) = 0, \quad \nabla\cdot\mathbf{u}_n = 0, \quad \mathbf{u}_n\cdot\mathbf{n}|_{\partial\mathcal{D}} = 0, \quad (4.7c)$$

where $\mathbf{u}^*_n = 2\mathbf{u}_{n-1} - \mathbf{u}_{n-2}$ is a second-order approximation to $\mathbf{u}_n$, and c^*_n, κ^*_n are defined similarly. The stability of the above scheme can be established by using essentially the same procedure as in the last subsection. However, it does involve tedious technical detail that we shall leave to interested readers.

4.3. **Spectral-Galerkin method in space.** In practice the coupled linear elliptic system for $(\tilde{\mathbf{u}}_n, c_n)$ in (4.7) is solved by either an iterative solver with a block diagonal preconditioner or by a decoupled approach, with approximations to all nonlinear terms are treated explicitly. Therefore, at each time step, we need to solve a sequence of vector and scalar Poisson-type equations for $\tilde{\mathbf{u}}_n$, c_n and p_n.

We shall use a spectral-Galerkin method [26, 17, 20] for solving these Poisson-type equations. More precisely, the equations are first decoupled into scalar Poisson-type equations for each Fourier mode in the azimuthal direction (see [14, 20]). The decoupling of the vector Poisson-type equation is non-trivial and is explained in more details here. The first two components of the vector Poisson-type equation reads:

$$\begin{aligned}\alpha u_r - \left(\Delta u - \frac{1}{r^2}u_r - \frac{2}{r^2}\frac{\partial u_\theta}{\partial \theta}\right) &= f_r,\\ \alpha u_\theta - \left(\Delta u_\theta - \frac{1}{r^2}u_\theta + \frac{2}{r^2}\frac{\partial u_r}{\partial \theta}\right) &= f_\theta,\end{aligned} \tag{4.8}$$

where α is a non-negative constant. Define the complex variables

$$\mathsf{u} = u_r + \mathsf{i}u_\theta, \quad \mathsf{f} = f_r + \mathsf{i}f_\theta.$$

Then the vector Poisson-type equation (4.8) becomes

$$\alpha\mathsf{u} - \left(\Delta - \frac{1}{r^2} + \frac{2\mathsf{i}}{r^2}\frac{\partial}{\partial\theta}\right)\mathsf{u} = \mathsf{f}. \tag{4.9}$$

Express the functions as Fourier series:

$$\mathsf{u}(r,\theta,z) = \sum_{m=-\infty}^{\infty} \hat{\mathsf{u}}_m(r,z)e^{im\theta}, \tag{4.10}$$

and similarly for f. Substituting the Fourier expansions into equation (4.9) and collecting the terms for each Fourier mode m, we find that $\hat{\mathsf{u}}_m(r,z)$ satisfies the following equations for $m \geq 0$:

$$\alpha\hat{\mathsf{u}}_{\pm m} - \Delta_{\pm m+1}\hat{\mathsf{u}}_{\pm m} = \hat{\mathsf{f}}_{\pm m},$$

where Δ_m is the reduced Laplace operator:

$$\Delta_m u := \frac{1}{r}\frac{\partial}{\partial r}\left(r\frac{\partial u}{\partial r}\right) - \frac{m^2}{r^2}u + \frac{\partial^2 u}{\partial z^2}.$$

The boundary conditions of the Fourier coefficients $\hat{\mathsf{u}}_m$ can be derived from equations (2.10) and (2.13) as follows:

$$\begin{aligned}&\text{On } r = 1: && \hat{\mathsf{u}}_{\pm m} = \hat{u}_{z,\pm m} = 0, && \forall m,\\ &\text{On } z = 0: && \hat{\mathsf{u}}_0 = \mathsf{i}\,g(r), &&\\ & && \hat{\mathsf{u}}_{\pm m} = \hat{u}_{z,\pm m} = 0, && m > 0,\\ &\text{On } z = \Gamma: && \hat{\mathsf{u}}_{\pm m} = \hat{\mathsf{h}}_{\pm m}, \quad \hat{u}_{z,\pm m} = 0, && \forall m,\end{aligned}$$

where $\hat{\mathsf{h}}_m$ is the m-th Fourier coefficient of

$$\mathsf{h} = \frac{1}{Ca}\left(\frac{\partial\sigma}{\partial r} + \frac{\mathsf{i}}{r}\frac{\partial\sigma}{\partial\theta}\right).$$

5. **Numerical results.** The nonlinear equation of state $\sigma = \sigma(c)$ used in the computations is a fit to the experimentally measured surface tension of vitamin K_1 on a water substrate [9]. The fit has the form

$$\sigma(c) = \frac{a_2 + a_3c + a_4c^2}{1 + \exp(a_0a_1 - a_1c)} + \frac{a_5 + a_6c^2}{1 + \exp(a_1c - a_0a_1)},$$

where $a_0 = 1.108$, $a_1 = 32.37$, $a_2 = 20.11$, $a_3 = 97.04$, $a_4 = -45.9$, $a_5 = 72.4$ and $a_6 = -0.15$. In Figure 2, we plot the equation of state $\sigma(c)$.

Note that the Taylor expansion of σ at 0 is

$$\sigma(c) \sim 72.4 - 4.2\times10^{-13}c - 0.15c^2 - 6.5\times10^{-11}c^3 - 4.95\times10^{-10}c^4 - 3\times10^{-9}c^5 + \cdots.$$

In this case, we can take $\alpha = 0.15/2$ in (3.6). Thanks to the maximum principle satisfied by the concentration equation and that the range of interested values for

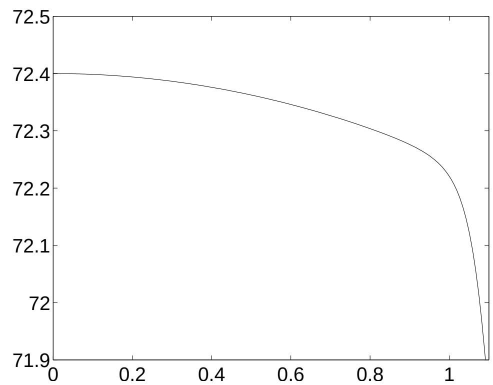

FIGURE 2. Surface tension as a function of surfactant concentration.

c is $[0, 1]$, we find that the condition (3.6) is satisfied by a large range of values of interest for Pe^s and Ca, including in particular the following parameters used in all our simulations:

$$Pe^s = 1000, \quad Ca = 0.001.$$

Other modeling and computational parameters are $\epsilon = 0.005$, $\gamma = 10^{-6}$, $\Delta t = 0.001$ with resolution (128, 32, 32) in the r- and z- and θ- directions, respectively.

5.1. **Base flow.** Note that the system is $SO(2)$ invariant, i.e., invariant under arbitrary rotations about the axis. As such, the base flow is axisymmetric and steady. Figure 3 shows the surfactant concentration and radial velocity on the free surface for $c_0 = 0.4\,\mathrm{mg\,m^{-2}}$ and $Re = 1000$. The results are similar to those in Lopez and Hirsa [18] and Hirsa et al. [9], though the flow in an annular region was considered in these two studies. Note that the surfactant is driven towards the axis, resulting in a region free of surfactant near the boundary. Figure 4 shows the streamlines and vortex lines (contours of ru_θ) in the meridional plane $(r, z) \in [0, 1] \times [0, \Gamma]$, where the axis is located on the left. The *Stokes stream function* ψ is defined through

$$u_r = -\frac{1}{r}\frac{\partial \psi}{\partial z}, \quad u_z = \frac{1}{r}\frac{\partial \psi}{\partial r}.$$

The streamlines and vortex lines show that the flow is essentially in solid-body rotation (i.e., $u_\theta \sim r$) for $r < 0.3$, with zero meridional motion ($\psi \sim 0$). The discontinuities between the stationary cylinder and the rotating bottom disk result in all the vortex lines that originate on the rotating bottom disk for $r > 0.6$ terminating at the discontinuities. This results in significant vortex line bending which induces the secondary meridional flow, as indicated by the streamlines.

5.2. **Primary instabilities.** For $c_0 = 0.4\,\mathrm{mg\,m^{-2}}$, the basic state remains stable up to about $Re = 1050$, at which point it loses stability via a supercritical Hopf bifurcation to an azimuthal mode with wavenumber $m = 3$. Contours of the surfactant concentration and the z-vorticity on the interface for $Re = 2000$ are shown in Figure 5, where the z-vorticity is defined as

$$\nabla \times \mathbf{u} \cdot \hat{\mathbf{z}} = \frac{\partial u_\theta}{\partial r} - \frac{1}{r}\left(\frac{\partial u_r}{\partial \theta} - u_\theta\right).$$

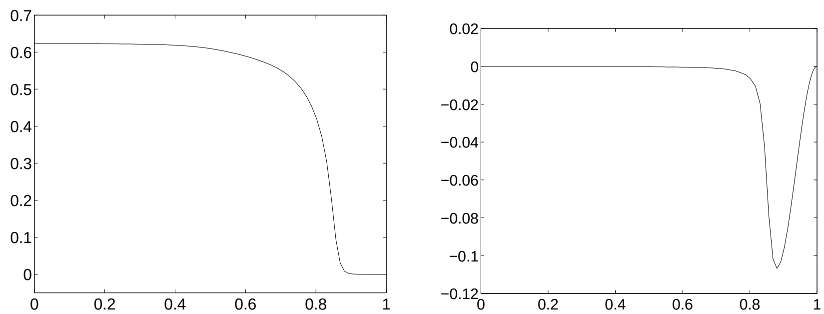

FIGURE 3. Results for $c_0 = 0.4\,\mathrm{mg\,m^{-2}}$ and $Re = 1000$: surfactant concentration (left) and radial velocity (right) on the free surface.

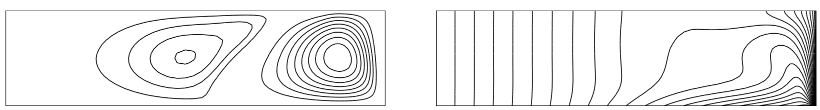

FIGURE 4. Results for $c_0 = 0.4\,\mathrm{mg\,m^{-2}}$ and $Re = 1000$. Streamlines (left) and vortex lines (right) in the meridional plane. Contour levels of vertex lines are spaced quadratically.

Note that clearing of surfactant occurs near the boundary. This mode is a rotating wave with non-dimensional period $t = 3.334$, which agrees well with the experimental result of Vogel et al. [33].

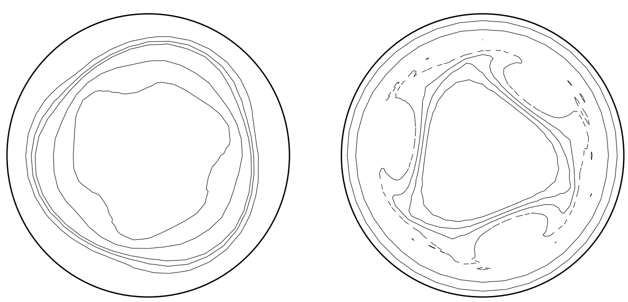

FIGURE 5. Results for $c_0 = 0.4\,\mathrm{mg\,m^{-2}}$ and $Re = 2000$. Left: contours of surfactant concentration at 0.05, 0.4, 0.5, 0.6, 0.65 ($\mathrm{mg\,m^{-2}}$). Right: contours of z-vorticity at -2, -1, 0, 0.5, 1, 1.5.

6. **Concluding remarks.** We have studied a mathematical model for a system of an incompressible flow with an insoluble surfactant on the top of a cylinder when the flow is driven by the constant rotation of the bottom wall. By making a reasonable assumption on the equation of state, we have established existence of a global weak solution for the coupled nonlinear system for the fluid velocity, pressure and surfactant concentration. We have also constructed efficient time-discretization scheme, that leads to a coupled linear elliptic equation for the velocity

and concentration and a Poisson equation for the pressure at each time step, and proved that the scheme is essentially unconditionally stable..

We have implemented a numerical scheme which consists of a second-order rotational pressure correction scheme in time and spectral-Galerkin methods in space, and use it to simulated the monolayer dynamics with equation of the state for the surface tension compatible with the experiment done by Hirsa et al. [9]. We investigated the dependence of Reynolds number Re on the stability of the base flow. From numerical results, we found that there exists a series of symmetry breaking into several azimuthal modes and some of these modes are unstable with respect to three-dimensional perturbations. With a low surfactant concentration $c_0 = 0.4\,\mathrm{mg\,m^{-2}}$, numerical simulations showed clearing of surfactant near the boundary wall. The three-dimensional results are in agreement with the experimental result of Vogel et al. [33].

Acknowledgments. The authors would like to thank Professors A. Hirsa and J. Lopez for suggesting this work and for many stimulating discussions. The work of J. Shen is partially supported by grants NSF 0915066 and AFOSR FA9550-08-1-0416.

REFERENCES

[1] A. W. Adamson and A. P. Gast, "Physical Chemistry of Surfaces," John Wiley & Sons, Inc., sixth ed., 1997.

[2] J. Boussinesq, *Existence of a superficial viscosity in the thin transition layer separating one liquid from another contiguous fluid*, C. R. Hehd. Seances Acad. Sci., **156** (1913), 983–989.

[3] M. Brøns, L. K. Voigt and J. N. Sørensen, *Topology of vortex breakdown bubbles in a cylinder with a rotating bottom and a free surface*, J. Fluid Mech., **428** (2001), 133–148.

[4] O. Daube, *Numerical simulation of axisymmetric vortex breakdown in a closed cylinder*, in "Vortex Dynamics and Vortex Methods," American Mathematical Society, 1991, 131–152.

[5] J. Dusting, J. Sheridan and K. Hourigan, *Flows within a cylindrical cell culture bioreactor with a free-surface and a rotating base*, in "Proceedings of the 15th Australasian Fluid Mechanics Conference," University of Sydney, M. Behnia, W. Lin and G. D. McBain, eds., 2004.

[6] ———, *A fluid dynamics approach to bioreactor design for cell and tissue culture*, Biotechnol. Bioeng., **94** (2006), 1196–1208.

[7] J. B. Grotberg, *Pulmonary flow and transport phenomena*, Annu. Rev. Fluid. Mech., **26** (1994), 529–571.

[8] J. L. Guermond and J. Shen, *On the error estimates for the rotational pressure-correction projection methods*, Math. Comp., **73** (2004), 1719–1737.

[9] A. H. Hirsa, J. M. Lopez and R. Miraghaie, *Measurement and computation of hydrodynamic coupling at an air/water interface in the presence of an insoluble monolayer*, J. Fluid Mech., **443** (2001), 271–292.

[10] ———, *Symmetry breaking to a rotating wave in a lid-driven cylinder with a free-surface: Experimental observation*, Phys. Fluids, **14** (2002), 29–32.

[11] A. H. Hirsa, J. M. Lopez, M. J. Vogel and J. J. F. Leung, *Effects of shearing flow with inertia on monolayer mesoscale structure*, Langmuir, **22** (2006), 9483–9486.

[12] J. M. Hyun, *Flow in an open tank with a free surface driven by the spinning bottom*, J. Fluids Eng., **107** (1985), 495–499.

[13] R. Iwatsu, *Numerical study of flows in a cylindrical container with rotating bottom and top flat free surface*, J. Phys. Soc. Jpn., **74** (2005), 333–344.

[14] Y.-Y. Kwan, "Fast Spectral Methods for Incompressible Flows," PhD thesis, Purdue University, 2008.

[15] ———, *Efficient spectral-Galerkin methods for polar and cylindrical geometries*, Appl. Num. Math., **59** (2009), 170–186.

[16] F.-C. Li, M. Oishi, Y. Kawaguchi, N. Oshima and M. Oshima, *Experimental study on symmetry breaking in a swirling free-surface cylinder flow influenced by viscoelasticity*, Exp. Therm. Fluid Sci., **31** (2007), 237–248.

[17] J. Lopez and J. Shen, *An efficient spectral-projection method for the Navier-Stokes equations in cylindrical geometries I. Axisymmetric cases*, J. Comput. Phys., **139** (1998), 308–326.

[18] J. M. Lopez and A. Hirsa, *Surfactant influenced gas/liquid interfaces: Nonlinear equation of state and finite surface viscosities*, J. Colloid Interface Sci., **229** (2000), 575–583.

[19] J. M. Lopez, F. Marques, A. H. Hirsa and R. Miraghaie, *Symmetry breaking in free-surface cylinder flows*, J. Fluid Mech., **502** (2004), 99–126.

[20] J. M. Lopez, F. Marques and J. Shen, *An efficient spectral-projection method for the Navier-Stokes equations in cylindrical geometries. II. Three-dimensional cases*, J. Comput. Phys., **176** (2002), 384–401.

[21] R. McOwen, "Partial Differential Equations: Methods and Applications," Prentice Hall Inc., Upper Saddle River, New Jersey, 1996.

[22] A. J. Milani and N. J. Koksch, "An Introduction to Semiflows," vol. **134** of Monographs & Surveys in Pure & Applied Math, Chapman & Hall/CRC, 2005.

[23] R. Miraghaie, J. M. Lopez and A. H. Hirsa, *Flow induced patterning at the air-water interface*, Phys. Fluids, **15** (2003), L45–L48.

[24] J. C. Scott, *The preparation of water for surface-clean fluid mechanics*, J. Fluid Mech., **69** (1975), 339–351.

[25] L. E. Scriven, *Dynamics of a fluid interface*, Chem. Engng. Sci., **12** (1960), 98–108.

[26] J. Shen, *Efficient spectral-Galerkin method I. direct solvers for second- and fourth-order equations by using Legendre polynomials*, SIAM J. Sci. Comput., **15** (1994), 1489–1505.

[27] J. C. Slattery, L. Sagis and E.-S. Oh, "Interfacial Transport Phenomena," Springer, 2nd ed., 2007.

[28] S. A. Snow, U. C. Pernisz and R. E. Stevens, *Thin liquid model polyurethane films*, in Proceedings of the 1998 Polyurethane World Congress, 1999, p. C4.

[29] A. Spohn, M. Mory and E. J. Hopfinger, *Observations of vortex breakdown in an open cylindrical container with a rotating bottom*, Exp. Fluids, **14** (1993), 70–77.

[30] ———, *Experiments on vortex breakdown in a confined flow generated by a rotating disc*, J. Fluid Mech., **370** (1998), 73–99.

[31] H. A. Stone, *A simple derivation of the time-dependent convective-diffusion equation for surfactant transport along a deforming interface*, Phys. Fluids, **2** (1990), 111–112.

[32] R. Temam, "Navier-Stokes Equations: Theory and Numerical Analysis," AMS Chelsea Publishing, 2001.

[33] M. J. Vogel, R. Miraghaie, J. M. Lopez and A. H. Hirsa, *Flow-induced patterning of langmuir monolayers*, Langmuir, **20** (2004), 5651–5654.

[34] D. L. Young, H. J. Sheen and T. Y. Hwu, *Period-doubling route to chaos for a swirling flow in an open cylindrical container with a rotating disk*, Exp. Fluids, **18** (1995), 389–392.

Received March 2010; revised March 2010.

E-mail address: tkwan@tulane.edu
E-mail address: park196@math.purdue.edu
E-mail address: shen@math.purdue.edu